Food Research International 176 (2024) 113792

Contents lists available at ScienceDirect

Food Research International

journal homepage: www.elsevier.com/locate/foodres

Fluorescence lifetime imaging microscopy as a tool to characterize spice powder variations for quality and authenticity purposes: A ginger case study

Qing Han [a,c], Sara W. Erasmus [a], Arjen Bader [b], Christos Fryganas [a], Christopher T. Elliott [c,d], Saskia M. van Ruth [a,c,e,*]

[a] Food Quality and Design Group, Wageningen University & Research, P.O. Box 17, 6700 AA, Wageningen, the Netherlands
[b] Department of Agrotechnology and Food Sciences, Wageningen University & Research, 6708 PB, Wageningen, the Netherlands
[c] Institute for Global Food Security, Biological Sciences, 19 Chlorine Gardens, Queen's University Belfast, BT9 5DL, Belfast, Northern Ireland, United Kingdom
[d] School of Food Science and Technology, Faculty of Science and Technology, Thammasat University, 99 Mhu 18, Phahonyothin Road, Khong Luang, Pathum Thani 12120, Thailand
[e] School of Agriculture and Food Science, University College Dublin, Dublin 4, Ireland

ARTICLE INFO

Keywords:
Composition
Fluorescence lifetime
Food authentication
Food powder
Food quality
Phasor plot

ABSTRACT

Spices are usually ground for applications and the resulting particle size of the powders is an important product attribute in view of the release of flavour. However, inhomogeneity of the original material may lead to variations in the physicochemical characteristics of the particles. This variation and its linkage to particle size may be examined by particular imaging techniques. This study aimed to explore the potential of Fluorescence Lifetime Imaging Microscopy (FLIM) to characterize spice powders according to particle size variations and correlation with their pigment contents to reveal the chemical information contained within the FLIM data. Ginger powder was used as a representative powder model. The FLIM profiles of the individual samples and populations revealed that FLIM coupled with the phasor approach has the capacity to characterize spice powder according to particle size. Meanwhile, Principal Component Analysis of pre-processed FLIM data revealed clustering of particle size groups. Further correlation analysis between the pigment compound contents and FLIM data of the ginger powders indicated that FLIM reflected chemical information of ginger powder and was able to visualize endogenous fluorophores. The current study revealed the potential of FLIM to characterize ginger powder particles. This approach may be extrapolated to other spice powder products. The new knowledge is a step further in paving the way for the application of innovative techniques, already prevalent in other domains, to food quality and authentication.

1. Introduction

Ginger is one of the most popular spice products because of its refreshing woody aroma and pungent taste. The powdered form is one of the most common physical forms of ginger products. The quality and authentication of ginger powder are highly associated with the price of ginger powder and the safety of the consumers. For powdered form spice, the processing includes many steps, such as cutting, drying and most importantly grinding (Ramesh et al., 2001). The processing procedure significantly affects the physicochemical properties of spice powder (Dhiman & Prabhakar, 2021; Gao et al., 2020). Hence, characterizing the variations of spice products generated during food processing has always been an important topic to the food industry and food scientists. According to previous studies, the compositional and morphological differences caused by food processing can directly influence the fluorescence characteristics of the food product (Karoui & Blecker, 2011; Wang et al., 2020). A previous study that used fluorescence spectroscopy to analyse ginger slices treated with different preprocessing methods revealed the possibility of using fluorescence-based methods to characterize the variations of ginger products

Abbreviations: FLIM, fluorescence lifetime imaging; PCA, principal component analysis; HPLC, high-performance liquid chromatography; PTFE, polytetrafluoroethylene.

* Corresponding author at: Food Quality and Design Group, Wageningen University and Research, P.O. Box 17, 6700 AA, Wageningen, the Netherlands.
E-mail address: saskia.vanruth@ucd.ie (S.M. van Ruth).

https://doi.org/10.1016/j.foodres.2023.113792
Received 10 October 2023; Received in revised form 23 November 2023; Accepted 2 December 2023
Available online 4 December 2023

caused by food processing (An et al., 2020). Therefore, it would be of great interest to investigate the changes in fluorescence characteristics of ginger powder caused by physicochemical variations generated during processing.

The application of fluorescence-based techniques in food analysis has been explored due to the advantage of their non-invasive and high-sensitivity nature (Ahmad et al., 2017). A recent review by Sikorska and Khmelinskii (2016) introduced the application of fluorescence and chemometrics in food science, in which, the strong ability of fluorescence in food quality and authentication was discussed. Application such as the quantitative determination of chemicals and discrimination of food origin were included. The core concept of techniques based on fluorescence is to exploit the different properties of the fluorescence emission of auto-fluorescent molecules to study and analyse the biological structures and processes (Coling & Kachar, 1998). Various fluorescence parameters can be used in this approach, such as intensity, spectra and lifetime (Digman et al., 2008).

Fluorescence Lifetime Imaging Microscopy (FLIM) is a powerful method that can produce spatially resolved images of fluorescence lifetime to identify fluorophores or to investigate their local environment (Chang et al., 2007). It is added as a functionality to e.g. a confocal or multiphoton microscope. The application of the fit-free phasor approach allows to simplify the FLIM data analysis and provides a graphical global view of the fluorescence decay occurring at each pixel and/or in each image on a phasor plot (Stringari et al., 2011). The purpose of the phasor approach is to characterize the variations in the types and concentration of fluorescence compounds in samples using the reciprocity principle (Malacrida et al., 2021). The phasor approach converts a pixel with distinctive fluorescence decays (distinctive concentration distribution of fluorescence compounds in the pixel) into a phasor point in the universal semicircle with the real part of the Fourier transform of the fluorescence impulse response (g) and the imaginary part of the Fourier transform of the fluorescence impulse response (s) as coordinates (Digman et al., 2008). The universal semicircle in the phasor plot is the geometrical representation of the relative modulation of the emission (M) and angular delay (ϕ) (Malacrida et al., 2021). The fluorescence lifetime decreases along the semicircle from left to right (Geverts et al., 2014). The mathematical relationships between M, ϕ, g and s were defined by Weber (1981). The location of a phasor point, which means the value of g and s of the point, is determined by the distinctive concentration distribution of fluorescence compounds of the pixel. Plotting together all phasor points converted from the pixels, a phasor cloud of the sample is generated. By observing the distribution tendency of the distribution of all phasor points which means the size and shape of the phasor cloud, the variations of fluorescence compounds in different samples can be characterized (Malacrida et al., 2021). Even though FLIM coupled with the phasor approach has been widely applied in other life science fields, there are very few studies to revealed the potential application of FLIM in the food science domain (Chang et al., 2007; Marcu, 2012). In this study, ginger was used as an example to investigate the potential of using FLIM to characterize spice powder variations. The particle size of ginger powder was introduced as a starting point of variations generated during processing, since particle size is one of the most important variables generated during the grinding stage and is considered as an influential factor on ginger properties (Archana et al., 2021; Han et al., 2023).

The aim of present study was to explore the possibility of using FLIM to characterize ginger powder with different particle sizes. To achieve this, the following approach was taken. Fifteen authentic/original ginger powder samples were assigned to particle size groups based on their particle size distributions. These 15 samples were then further manually fractionated into smaller and larger-sized particle fractions to limit other potential influential variables between groups. The reason to classify the sample and conduct fractionation instead of pulverizing the same batch of ginger samples into different particle sizes is due to the fact that the grinding process in the laboratory is different from the grinding/processing in the industry. Additional variances might be introduced and create an impact on the original characteristics of the commercial samples. All ginger powder samples and their fractions were subjected to FLIM. Like other spectroscopy-based techniques, the FLIM profile reflects the chemical compositional information of the sample. However, as yet, no study has systematically summarized the overall fluorescence-exhibited compounds in ginger and their content. To determine the relationship between the FLIM profile and the chemical composition of ginger powder as well as the influence caused by particle size on the FLIM profile, in our study, three pigment compounds (curcumin, demethoxycurcumin and 1-dehydro-6-gingerdione) previously reported in ginger were selected for quantitative analysis, in order to reflect the chemical information of ginger powder back to its FLIM profile (Yoko & Aya, 2014). This selection was based on the fact that these three pigment compounds belong to the polyphenol group and the derivatives which exhibit fluorescence and some studies have indicated an influence of particle size on the colour of food powder samples (Nasef et al., 2019; Vidot et al., 2019; Zhao et al., 2010). Therefore, all ginger powder samples and their fractions were subjected to quantitative analysis of the pigment compounds' contents to reveal the relationship between the fluorescence lifetime profile, particle size and pigments content of the powders.

2. Materials and methods

2.1. Samples

Fifteen ginger powder samples, each sample originating from a different batch were used in this study. The authentic/original samples were acquired from two trustable European spice companies, one company provided ten samples and the other provided five samples. All samples were stored in plastic Ziplock® bags in a dark container in a refrigerator at 4 °C before further analysis.

2.2. Chemicals

Methanol and acetonitrile (HPLC grade) were purchased from Actu-All Chemicals b.v. (Oss, Netherlands). Formic acid (LC-MS grade) was purchased from HiPerSolv CHROMANORM® (Lutterworth, United Kingdom). Milli-Q water was obtained by using a water purification system (PURELAB flex 1, ELGA, Lane End, United Kingdom). Analytical standards of curcumin and demethoxycurcumin were purchased from Supelco (Amsterdam, Netherlands). The analytical standard of 1-dehydro-6-gingerdione was purchased from ChemFaces (Wuhan, China).

2.3. Particle size measurement

The particle size distribution of all samples (15 original samples and their fractions after sample fractionation) was analysed using a laser diffraction analyser coupled with an Aero S dry dispersion accessory (Mastersizer 3000, Malvern Instruments, Malvern, UK) based on the Fraunhofer diffraction theory (Keck & Müller, 2008). The settings of the analyser were as follows: 3 mm hopper gap of the dispersion accessory, two bar pressure and 100 % feed rate of the vibrational feeder. Three parameters were used to characterize the particle size of ginger powder, i.e., Dx 10, Dx 50 and Dx 90. The detailed explanations of three parameters are as follows: Dx 10 is the point at which 90 % of the sample particles above this point and 10 % of the sample particles below this point; Dx 50 is the point at which half of the sample particles above this point and half of the sample particles below this point; Dx 90 is the point at which 10 % of the sample particles above this point and 90 % of the sample particles below this point (van Ruth et al., 2019). All samples were measured in triplicate and values were averaged for each sample.

2.4. Sample fractionation and coding

A hierarchical cluster analysis was conducted to classify the 15 original ginger powders into three different particle size groups using the results of the particle size distribution of the samples acquired from section 2.3. Three particle size groups were small, medium and large particle size groups which were coded as Group I, II and III. The sample fractionation was conducted by dividing each sample into two fractions by sieving. The sizes of laboratory sieves were 75, 125 and 250 μm which were decided by the particle size parameter, Dx 50, of the three groups determined in section 2.3. By using Dx 50 as the dividing line, the volumes of smaller and larger-sized particle fractions would be approximately the same. The smaller-size particle fraction from Group I was coded as Group A and larger-sized particle fraction was coded as Group B. For Group II, smaller-sized particle fraction was coded as Group C and larger-sized particle fraction was coded as Group D. While the smaller-sized particle fraction from Group III was coded as Group E and larger-sized particle fraction was coded as Group F. Ultimately, Groups A, C and E represented small particle size fractions and Groups B, D and F represented large particle size fractions. A total of 30 fractions resulted from the sample fractionation. All samples and fractions (n = 45) were subjected to particle size measurement, FLIM and quantitative analysis of pigment compounds. Appendix Fig. 1 shows the schematic overview of the sample fractionation and sample coding.

2.5. Instrumentation and experimental procedure of FLIM

The fluorescence lifetime images of ginger powder samples were acquired using a Leica SP8 Dive multiphoton confocal imaging microscope (Leica Microsystems, Wetzlar, Germany). Before each measurement, the sample was placed on a microscope cover glass (24 × 50 mm, 170 ± 5 μm) using a laboratory micro sampling spoon with one spoon per sample. The samples were excited by an 80 MHz multiphoton excitation laser source at 800 nm with a 10X, 0.3 N.A dry objective lens (Leica Microsystems, Wetzlar, Germany). The image scan speed was 4 μs/pixel with an image size of 512 × 512 pixels. Optimal lifetime images were obtained by accumulating 60 images. Three areas were randomly imaged for each sample which generated three FLIM images per sample.

2.6. The quantitative analysis of pigment compounds in ginger powder

2.6.1. Preparation of ginger extraction and standard solutions

The extraction of each ginger powder was performed by weighing 0.5 g of samples into a 15 mL centrifuge tube and then adding 3 mL methanol. The mixture was fully vortexed and then ultrasonicated for 60 min at room temperature (20 °C). After centrifuging at 2000 × g for 5 min at 20 °C, the supernatant was collected. The solid residue was added to 3 mL methanol and repeated the extraction for two more times. The collected supernatant from the three extractions was then dried under Nitrogen in 15 mL centrifuge tubes and redissolved using methanol to 0.5 mL. The redissolved supernatants were filtered through a 0.2-μm polytetrafluoroethylene (PTFE) membrane for further analysis. The standard solution (10 μg/mL) of curcumin and demethoxycurcumin was prepared by dissolving the two compounds together in methanol. The standard solution (1000 μg/mL) of 1-dehydro-6-gingerdione was prepared individually by dissolving the compound in methanol. The standard solutions were diluted to 1, 2, 3, 4 and 5 μg/mL (curcumin and demethoxycurcumin standard solution) and 100, 200, 300, 400 and 500 μg/mL (1-dehydro-6-gingerdione) respectively and filtered (0.2-μm PTFE membrane) for the calibration curves for quantitative analysis.

2.6.2. High-performance liquid chromatography - photodiode array analysis

The quantitative analysis of pigment compounds in ginger powder samples was performed on the Thermo Scientific™ - UltiMate™ 3000 LC Systems (Thermo Fisher Scientific, Waltham, USA). The separations were carried out on an InfinityLab Poroshell 120 Ec-C18 column (2.1 × 50 mm, 2.7 μm) which was connected to a InfinityLab Poroshell 120 EC-C18 guard column (2.1 x 5 mm, 2.7 μm) (Agilent Technologies, Santa Clara, CA, USA). The column temperature was set at 40 °C during analysis. A binary gradient elution system composed of (A) Milli-Q water (0.2 % formic acid) and (B) acetonitrile (0.2 % formic acid) was applied as follows: 0.0–1.0 min, 30 % B; 1.0–12.5 min, 30–50 % B; 12.5–12.6 min, 50–95 % B; 12.6–14.6 min, 95 % B; 14.6–14.7 min, 95–30 % B. Three minutes equilibration followed each run. The injection volume of each sample was 5 μL and the flow rate was 0.5 mL/min. A UV–visible diode array was set from 220 to 550 nm for acquiring chromatograms and the liquid chromatography profile at 420 nm for each sample were used for quantification analysis. The data acquisition and processing program were conducted using Chromeleon 7 software (Thermo Fisher Scientific, New York, USA). All samples were measured in triplicate and values were averaged for each sample.

2.7. Data processing and statistical analysis

Hierarchical cluster analysis with Ward's method and three cluster trees was conducted using the particle size distribution data of 15 ginger powder samples in RStudio (R Foundation for Statistical Computing, Vienna, Austria). Significance of differences in particle size distribution (Dx 10, Dx 50 and Dx 90) between Group I, II and III were evaluated

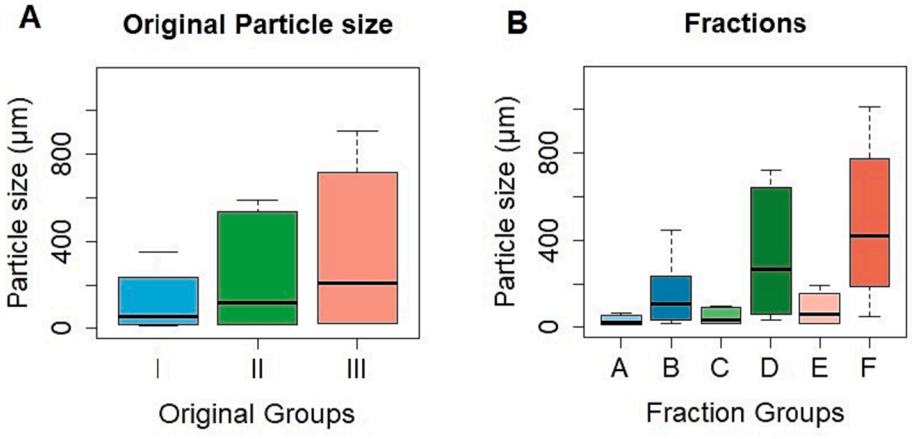

Fig. 1. Boxplots of the particle size distributions. (A) The three original ginger powder groups (Group I, II and III), (B) The six particle size fraction groups (Group A and B (from Group I), C and D (from Group II), and E and F (from Group III)). Note: The middle "box" represents the 50% of data in the group. The line across the box, is the median of the data set. The upper and lower whiskers represent the biggest and smallest particle size value in the group.

using the Kruskal-Wallis non-parametric test followed by multiple pairwise comparisons using the Steel-Dwass-Critchlow-Fligner procedure (two-tailed). $P < 0.05$ was considered statistically significant. The Kruskal-Wallis non-parametric test was chosen since the particle size data was not normally distributed nor with equal variance. The determination of the data distribution and homogeneity of variance were conducted by the Shaprio-Wilk test and Leven's test in SPSS (IBM SPSS Statistics 28.0.1, IBM, Armonk, NY, USA).

The FLIM image of each measurement was analysed using ImageJ, a free public-domain software developed by the National Institutes of Health (Gomez-Perez et al., 2016). The phasor plot of each measurement was generated in ImageJ by transforming all pixels of the FLIM image into phasor points in a universal circle as previously described by Malacrida et al. (2021) using an adapter version of the time-gated phasor plugin developed by Fereidouni (https://doi.org/10.1111/j.1365–2818.2011.03533.x). A comparative analysis of the phasor distribution of different groups was conducted by using the average *g* and *s* values of the phasor distribution of each measurement calculated by ImageJ and plotted together as a scatter plot in RStudio. In the scatter plot, each point represented one measurement. Besides the phasor approach, Principal Component Analysis (PCA), a common technique for interpreting the structure of data, was applied to FLIM data using RStudio. To facilitate PCA, the FLIM data were pre-processed using ImageJ. The fluorescence lifetime of each measurement was transformed into a histogram with a lifetime from 0 to 3 ns binned into 250 data segments as the X axis and the number of photons hit on the detector at each data segment on the Y axis respectively.

All chromatographic data were processed and interpreted in Chromeleon 7. Calibration curves were generated by linear regression of integrated peak areas and analytical standards of curcumin, demethoxycurcumin and 1-dehydro-6-gingerdione with known concentrations. With the linear regression equations of the calibration curves and the peak areas, the concentrations of the three pigment compounds in each sample were determined. Statistical analysis of the content of three pigment compounds was conducted by GraphPad Prism 8.0.2 (GraphPad Software, San Diego, CA, USA). The results of the content of three pigment compounds in different groups were presented as mean ± standard deviation (SD). Significance of differences in pigment compounds between Group I, II and III were evaluated using the Kruskal-Wallis non-parametric test followed by multiple pairwise comparisons using SPSS. $P < 0.05$ was considered statistically significant. The Kruskal-Wallis non-parametric test was chosen because the pigment concentrates results of samples were not normally distributed nor with equal variance. The determination of the data distribution and homogeneity of variance were conducted by the Shaprio-Wilk test and Leven's test in SPSS.

Additionally, Pearson correlation coefficients (r) were conducted to evaluate correlation between the fluorescence lifetime and the content of pigment compounds in ginger by RStudio since the Pearson correlation coefficient can provide insights into the degree and direction of linear correlation between the variables.

3. Results and discussion

3.1. Particle size distribution of the original ginger powders and their fractions

The overall distribution of particle size of the original 15 ginger powder can be seen in Appendix Table A1. To classify the ginger powder samples into different particle size groups, Dx 10, Dx 50 and Dx 90 of the samples were used as parameters to conduct the hierarchical cluster analysis (Fig. A.2). The cluster assigned samples numbered 1, 2, 3, 4 and 15 to Group I, samples numbered 10, 11, 12,13 and 14 to Group II, and samples numbered 5, 6, 7, 8 and 9 to Group III. The particle size distribution of the three original groups (Group I, II and III) are visually presented by boxplot in Fig. 1**A**. Except for the Dx 10 value of Group I and II, significant differences can be observed between all three groups for Dx 10, Dx 50 and Dx 90 values. As described in Section 2.4, all samples from the three original groups were separated into smaller and larger-sized particle fractions and measured by particle size distribution (Table A2). This sample fractionation generated six fraction groups, i.e., Group A and B (from Group I), Group C and D (from Group II) and Group E and F (from Group III). The particle size distributions of six fraction groups are shown in Fig. 1**B**. As can be seen from the Fig. 1**B**, this sample fractionation led to a more distinctive particle size distribution compared with the three original groups.

3.2. Three original groups: FLIM profiles and pigments content

In this section, the FLIM profiles and pigments content of three original groups (Group I, Group II and Group III) were investigated. Multiphoton excited fluorescence lifetime imaging microscopy and the phasor approach were employed to generate the FLIM profiles of individual samples and populations. Multiphoton excited fluorescence lifetime imaging microscopy is an imaging technique that provides spatially resolved information about fluorescent molecules with deeper penetration into the samples due to the less photodamage and less light scattering by using two photons of lower energy (Sánchez & Gratton, 2005). PCA was conducted to compare the phasor approach with the traditional food quality/authentication data interpretation method to provide an understanding of the phasor approach. In addition, the distribution of three pigment compounds (curcumin, demoxycurcumin and 1-hydro-6-gingerdione) was analysed using HPLC.

3.2.1. FLIM profiles of the three original groups

The multiphoton excited fluorescence lifetime images allow a straight-forward visualization of the particle size and the distribution of fluorescent molecules in ginger samples. As can be seen from Fig. 2**A**, similar to other common microscopy techniques, FLIM appears to be able to distinguish the three groups based on particle size appeared on the images (Strege et al., 2013). In addition, ginger powders in different particle sizes present similar fluorescence lifetime (as can be seen from the similar bright green false colour that corresponds to a fluorescence lifetime around 1 ns), indicating the similarity in the types and concentrations of the fluorescence compounds in general, except samples from Group III present bright blue dots in some areas (Fig. 2**A**).The variation in the fluorescence lifetime image of Group III means a difference in the types and/or concentration distribution of fluorescence compounds in Group III. The corresponding phasor plots further indicated a greater difference between Group III and Group I, II. According to the reciprocity principle on the phasor plot, the phasor positions of a phasor point is related to the position of the original fluorescence compounds contributing to the signal in each pixel and the relative contribution (concentration) of these fluorescence compounds (Malacrida et al., 2021). Therefore, the differences in the shape and size of the phasor clouds of samples indicate the variations in types and concentrations of fluorescence compounds in ginger. In this study, the phasor clouds of the three groups showed different patterns in terms of size and/or shape, especially for Group III. The phasor plots of the three original groups not only confirmed and further enlarged the difference in the types and/or concentration distribution of fluorescence compounds in Group III compared with the other two groups but also further indicated the difference between Group I and II which are not obvious in the FLIM images. Compared with the original fluorescence lifetime image, the phasor plot of individual samples provides a more straightforward way of visualizing the distribution of fluorescence compounds in food powder.

A comparative analysis of phasor distribution of all samples in the three original groups was conducted using the average *g* and *s* values of each sample. The result of the comparative phasor plot can be seen in Fig. 3**A**. The phasor distribution of the three original ginger powder groups displays a tendency of separation. Greater variations can be

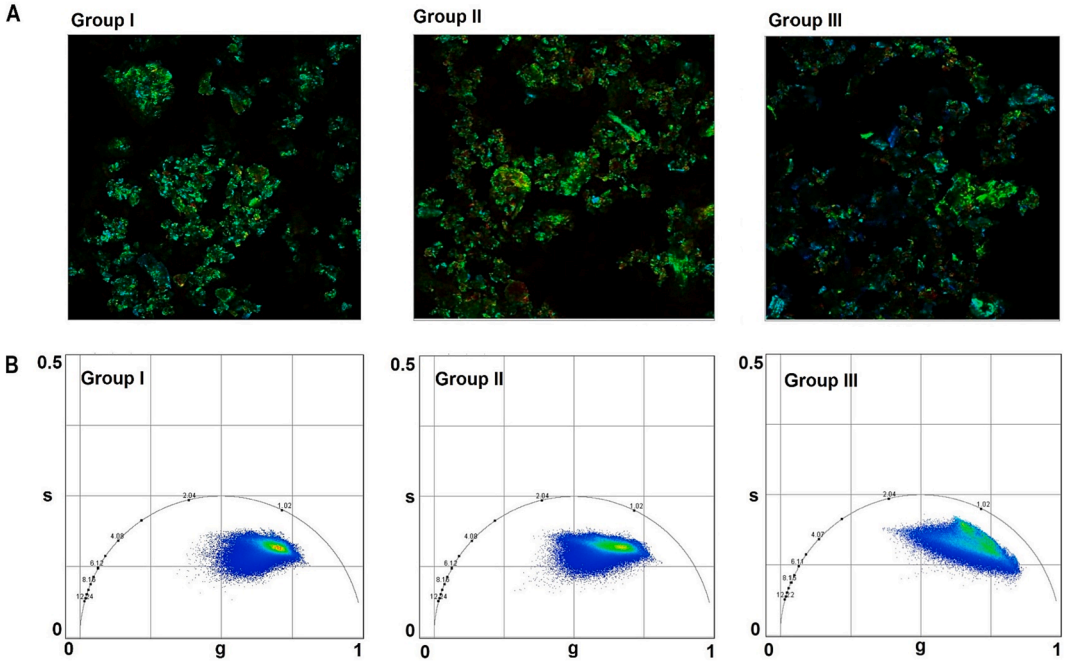

Fig. 2. Fluorescence lifetime images and corresponding phasor plots of the three original groups. (A) Fluorescence lifetime images of the three original groups, (B) Phasor plots of the three original groups.

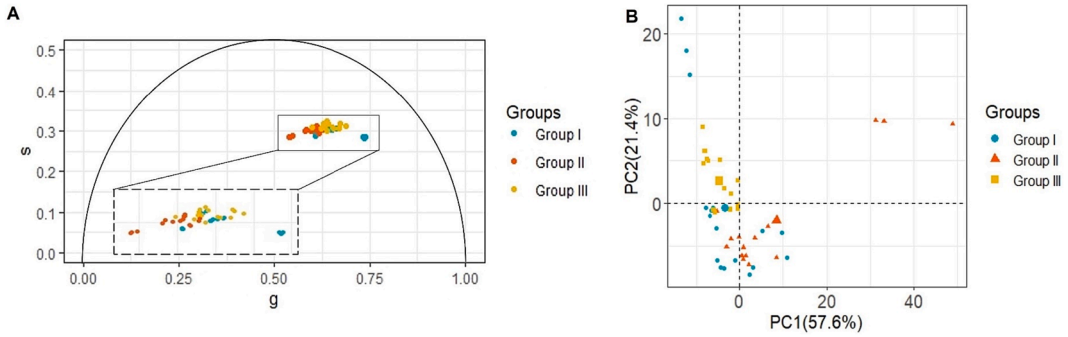

Fig. 3. (A) Comparative phasor distribution of the three original groups, (B) Principal Component Analysis (PCA) of the three original groups. Note: The dotted big rectangle in part (A) represents the zoom-in of the phasor distribution of samples.

observed along the *g* axis between Group II and the two other groups and the *s* axis between Group III and the two other groups (Fig. A.3**A**). However, the three groups are not clearly separated from each other. This could be because this comparative analysis was conducted using the average *g* and *s* values of each sample. Compared with the phasor plot generated using all pixels of each sample (Fig. 2**B**), detailed information might be limited/eliminated after averaging. The PCA was conducted using the pre-processed lifetime (data bin segments of the lifetime and the numbers of the photons hit on the detector at each data segment) of the samples to reduce dimensionality and visualize the structure of data (Rodarmel & Shan, 2002). Compared with the average *g* and *s* values used in the comparative analysis of phasor distribution, the dataset used for PCA contained more information. Fig. 3**B** shows the result of PCA of the three original groups. A separation can be observed between Group III and the two other groups along PC2 (explaining 21.4 % of the variation). The PCA plot is in line with the individual phasor plots of samples from the three groups in which a distinctive different size and shape of phasor cloud in Group III can be found (Fig. 2**B**). To summarize the information from Fig. 2 and Fig. 3, the results indicate that the FLIM combined with the phasor approach has a strong ability to characterize individual ginger powder samples at the particle level. In addition, pre-processed fluorescence lifetime data combined with chemometrics (PCA) showed a potential of discriminating spice powder with variations. Even though in PCA plot Group III was separated from Group I and II, the distribution of Group I and II overlapped. This result also suggests that the particle size might not be the only factor influencing the fluorescence lifetime profile of ginger powder as there could be other confounding factors.

Particle size is a natural variable generated during ginger powder production. Nevertheless, many other variables can also create considerable impact on the fluorescence exhibited compounds in ginger powder. For instance, the geographical origin of a food product has proved to be one of the most important reasons caused compositional differences of food products which could further affect the results of excitation–emission fluorescence spectra (Dupuy et al., 2005; Hao et al., 2021). Apart from the grinding step that has shown to cause variations in particle size in this study, other steps of ginger powder production may also potentially influence the FLIM profile, as each step introduces alterations to the chemical properties to some extent (Draszanowska et al., 2020; Sida et al., 2019). A study conducted on assessing the drying methods of ginger indicated that drying conditions had an effect on polyphenol content, where total polyphenol content decreased with increasing microwave output power (Kubra et al., 2012). Polyphenols are compounds that can exhibit fluorescence in food (Mekoue Nguela

et al., 2019). In addition, the ginger peeling step (peeling or unpeeling) could also influence the content polyphenols in ginger and might further influence its FLIM profile (Liang et al., 2023). The study observed a higher content of total polyphenol in unpeeled ginger compared with peeled ginger. The impact from drying is not limited to the polyphenols as the content of heat-sensitive vitamin Bs (i.e., pyridoxine, Riboflavin, Niacin and Thiamin), which are endogenous fluorophores that exist in ginger, might be also decreased or even destroyed by different drying conditions (Croce & Bottiroli, 2014; Fuliaş et al., 2014; Maslanka et al., 2018; Perry et al., 2012). Due to the heat-sensible nature, the cleaning step (various forms of thermal blanching) also influence vitamin Bs, and furthermore, the FLIM profile (Amoah et al., 2020).

3.2.2. *Pigments content of the three original groups*

The content of curcumin, demoxycurcumin and 1-dehydro-6-gingerdione which are the pigment compounds responsible for the yellow colour of ginger, in the three original ginger powder groups (Group I, Group II and Group III) are shown in Fig. 4**A**. The detailed results of each sample can be found in Table A3. For the three original groups, the contents of all three pigment compounds in Group III were significantly lower than Group I and Group II. There is no significant difference observed between Group I and Group II in terms of the three pigment compounds, despite the mean value of curcumin and demoxycurcumin in Group I were obviously higher than Group II in the figure. This is because one sample (sample no. 1) in Group I has a distinctive higher curcumin and demethoxycurcumin contents than other samples, see Table A3. The results of quantitative analysis of pigment compounds in the three original groups revealed the same information as the PCA plot of fluorescence lifetime data of the three original groups, i.e., Group I and II are similar while Group III is distinctive different from Group I and II. Like the FLIM profiles, there are other factors also influencing the variations in the pigment content in the three original ginger powder groups. According to previous studies, potential influential factors that contribute to the variation in pigment compounds in ginger could be genetic variations, environmental conditions, maturation, etc (Poudel et al., 2019; Tayyem et al., 2006; Vedashree et al., 2020; Verma et al., 2019; Yoko & Aya, 2014).

To summarise the information from the FLIM profiles and pigments content of the three original ginger powder groups, variations were observed in ginger powder samples with different particle sizes, but other underlying factors might also have had an influence. However, based on the original three groups, it is difficult to determine the impact of particle size and/or the extent of the impact. Therefore, in the next section, to limit the variable to the particle size only, the FLIM profiles and pigments content of the smaller and larger-sized particle fractions from the same original groups will be discussed since the only underlying variable is particle size.

3.3. *Six fraction groups: FLIM profiles and pigments content*

3.3.1. *FLIM profiles of the six fraction groups*

Multiphoton excited fluorescence lifetime images and their corresponding phasor transformations of the representatives of six fraction groups are displayed in Fig. 5. As can be seen from the fluorescence lifetime image in Fig. 5**A**, the ginger fractions also present bright green false colour as their corresponding original groups. Bright blue dots can be observed in both Group E and F (originated from Group III). In addition, fluorescence lifetime images exhibit a clear difference in particle size between the smaller and large-sized particle fractions from the same original group. For the individual phasor plots of the fraction samples, even though the size and shape of phasor clouds of the smaller and larger-sized particle fractions from the same original group are slightly different from each other, the differences from the original groups' perspective are more pronounced. The result indicated that the influences from other underlying factors (e.g., geographical origin and processing procedure) discussed in section 3.2.1 might be greater than particle size.

The results of the comparative analysis conducted on the six fraction groups are visually presented in Fig. 6. No clear grouping pattern between groups can be found from the phasor distribution of six fraction groups as the samples in most of the groups overlapped. Greater variations can be observed in Group C between other groups along the *g* and *s* axis (Fig. A.3**B**). This can also be seen from the more separated distribution of samples from Group C in the phasor plot (Fig. 6**A**). Even though there is no distinctive separation among the six fraction groups in the PCA plot (Fig. 6**B**), the distribution of smaller and larger-sized particle fractions from the same original group are clustered together. Furthermore, most of the samples from Group E and F (Group III) are clustered in the upper part of the plot and most of the samples from Group A, B, C and D (Group I and Group II) are in the lower part. This trend consistent with the PCA results of the three original groups (Fig. 3**B**). Fig. 7 shows the results of comparative phasor distribution and PCA of the smaller and larger-sized particle fractions from the same group. Notably, both for the phasor distribution and PCA, the samples of smaller and larger-sized particle fractions from the same original group, such as Group A and B from Group I, are overlapped with each other. Summarizing the results of Fig. 6 and Fig. 7, it is evident that the particle size of ginger powder had no or limited effect on the FLIM profile of ginger powder, implying that there was likely little or no change in the types and/or concentration distribution of fluorescence compounds due to particle size. For traditional spectroscopy techniques, the light scattering caused by particle size difference of samples needs to be corrected and/or compensated by data pre-processing (Hahn, 2009). However, whether the data pre-processing can fully remove the light scattering effect is still under debate (Rinnan, 2014; Thennadil & Martin, 2005; Wan et al., 2020; Wang et al., 2011). Compared with common spectroscopy techniques, the FLIM profile can avoid the light scattering effect and can interpret food powder from the particle level by generating a fluorescence lifetime image. In our previous study, an impact of particle size on high-resolution visual imaging and spectral imaging profiles has been demonstrated which emphasizes the importance of considering and evaluating internal sample variations before applying these techniques (Han et al., 2023). This study proved the considerable potential of utilizing FLIM to discern sample differences based on external variations, such as geographical origin, as the minimal influence caused by internal variation (particle size).

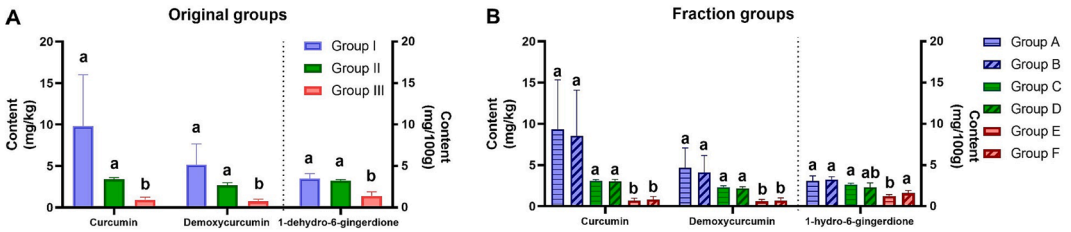

Fig. 4. Pigment compounds content in the three original groups and the six fraction groups. (A) Three original groups, (B) Six fraction groups.

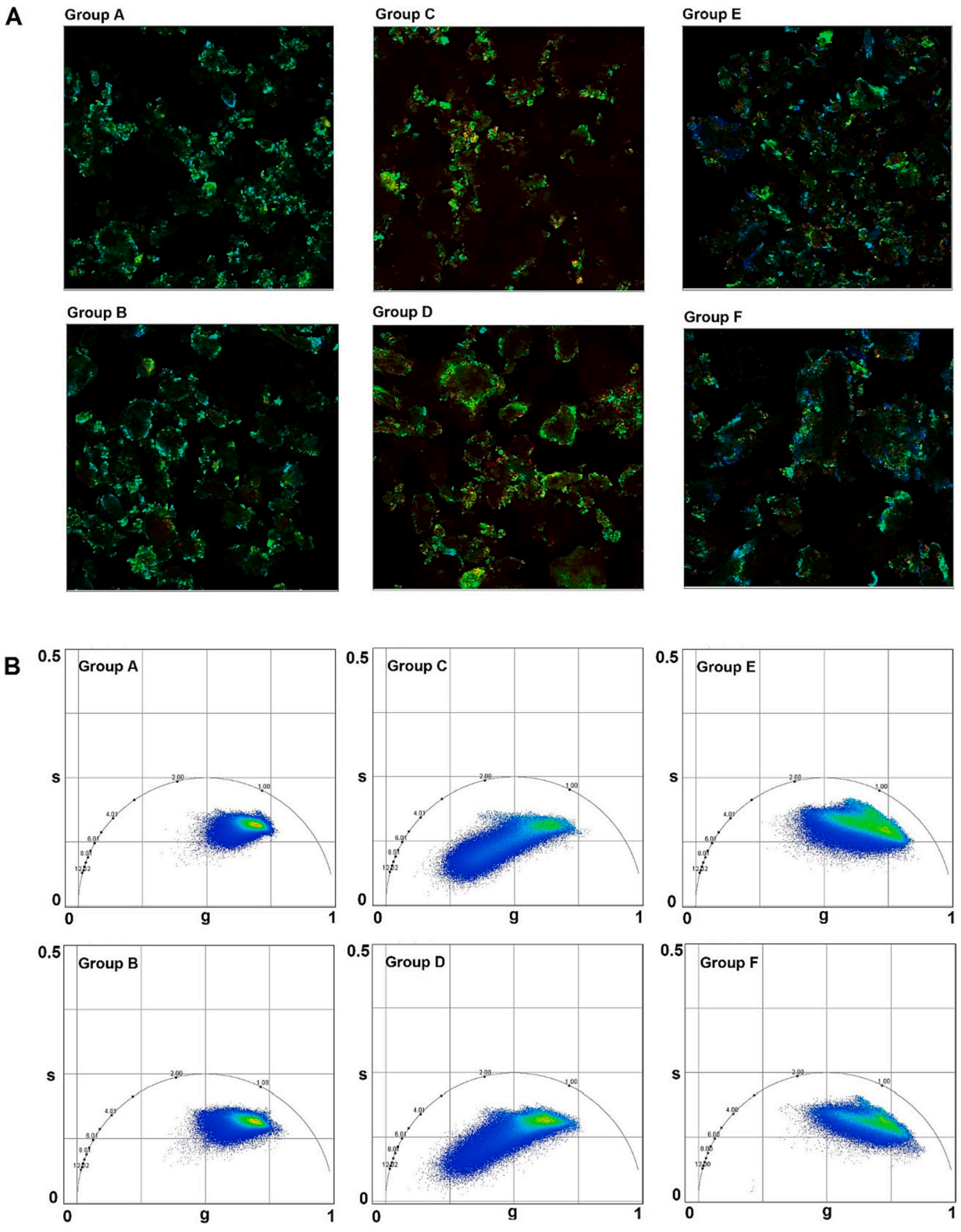

Fig. 5. Fluorescence lifetime images and corresponding phasor plots of the six fraction groups. (A) Fluorescence lifetime images of the six fraction groups, (B) Phasor plots of the six fraction groups.

3.3.2. Pigment content of the six fraction groups

The contents of three pigment compounds in the six fraction groups (Group A, B, C, D, E and F) are shown in Fig. 4**B**. For the six fraction groups, no significant difference can be found in the smaller-sized particle fraction and larger-sized particle fraction from the same sample. In addition, except for 1-dehydro-6-gingerdione in Group F, the pigment compounds in Group E and F (Group III) were significantly lower than in Group A-D (Group I and II). No significant difference can be found in all three pigment compounds between Group A-D (Group I and II). The result of fraction groups was in line with the original groups, which is Group III differed from the other two by itself. The higher mean value of curcumin and demethoxycurcumin in Group A and B can be attributed

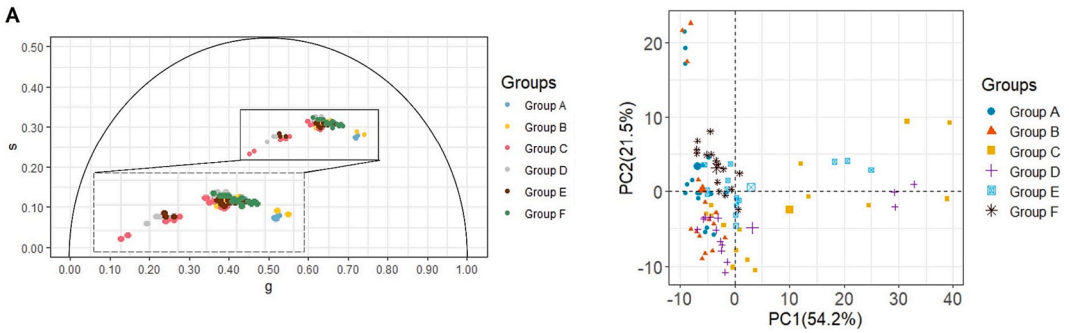

Fig. 6. (A) Comparative phasor distribution of the six fraction groups, (B) Principal component analysis (PCA) of the six fraction groups. Note: The dotted big rectangle in part (A) represents the zoom-in of the phasor distribution of samples.

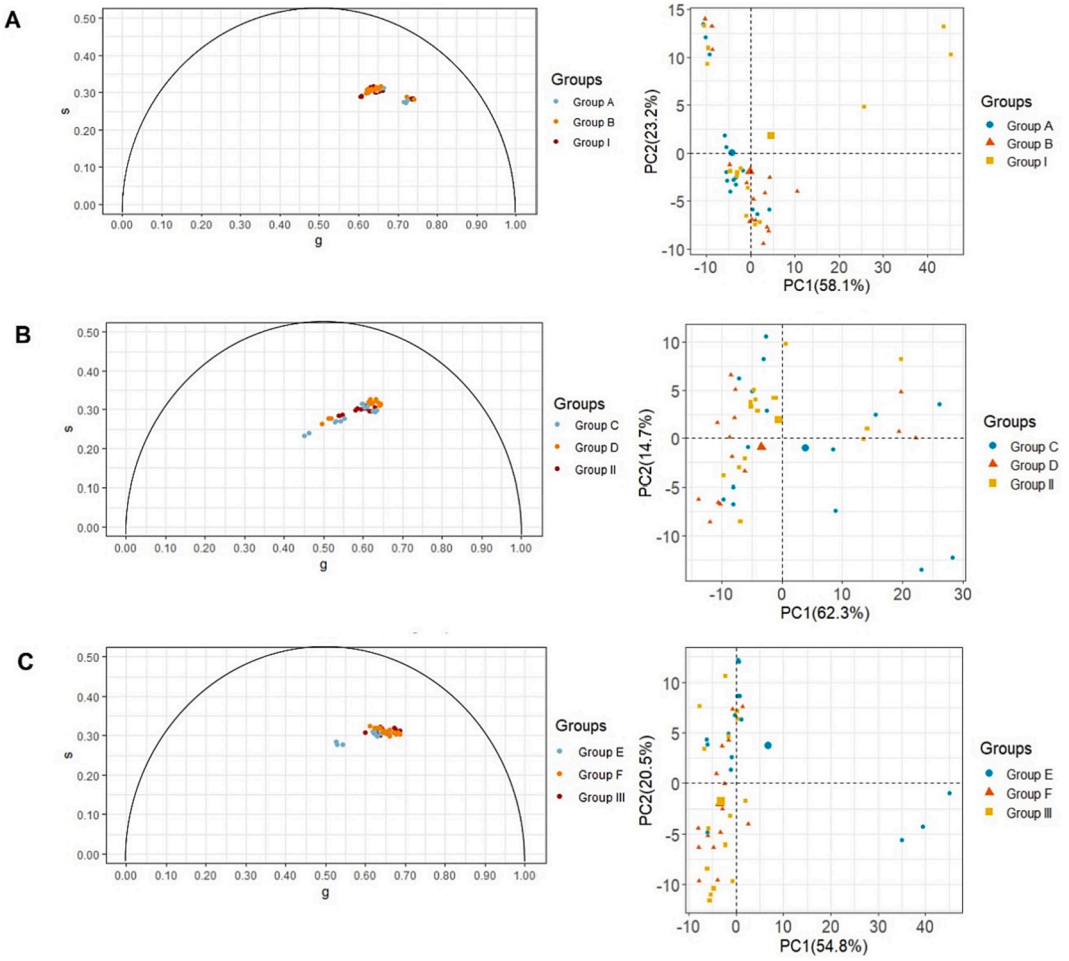

Fig. 7. Phasor distribution and PCA of six fraction groups and their corresponding original groups. (A) Group A, B and Group I, (B) Group C, D and Group II, (C) Group E, F and Group III.

to the same underlying reason as observed in the original groups, i.e., the presence of distinctly higher curcumin and demethoxycurcumin content in samples no. 1-S and 1-L (Table A4). The results of quantitative analysis of pigment compounds for fraction groups suggest that the particle size variations of ginger powder do not influence the concentrations of pigment compounds.

Even though the quantitative analysis of pigment compounds for ginger powders showed similar results as the FLIM data, no study has systematically summarized the overall fluorescence exhibited compounds in ginger. In addition, the three pigment compounds are only parts of the polyphenol groups, one cannot conclude that the three pigment compounds can be totally responsible for the variations in FLIM variations. However, it is possible to obtain an impression of the relationship between the pigment compounds and fluorescence lifetime by correlation analysis which can further determine if the types and concentrations of pigment compounds have contribution to the variations in FLIM variations. Therefore, in the next section, the correlation analysis is described to reveal the relationship between pigment compounds and fluorescence lifetime.

3.4. The relationship between the fluorescence lifetime and pigment compounds of ginger powder

The correlation analysis of fluorescence lifetime and pigment compounds in ginger powder was conducted using the *g, s* values generated by the phasor approach and concentration of the pigments. Fig. 8 shows the result of the correlation analysis. The result suggested the concentration of the three pigment compounds were highly correlated. However, only 1-dehydro-6-gingerdione was found positively correlated with the *s* value and negatively correlated with the *g* value. No clear correlation can be observed between the *g, s* value and the other two pigment compounds. The correlation between the fluorescence lifetime and 1-dehydro-6-gingerdione revealed that 1-dehydro-6-gingerdione is one of the fluorescence compounds that have a greater contribution to ginger powder's FLIM profile. 1-dehydro-6-gingerdione belongs to hydroxycinnamic acid which has been proven to have fluorescence exhibition properties in many studies (Rhodes et al., 2002; Stelzner et al., 2019; Vidot et al., 2019). It needs to be mentioned that ideally, a direct comparison with the reference compound would have been a validation. However, it would require the addition of 1-dehydro-6-gingerdione to ginger powder without further interfering compounds. It would be extremely difficult to mimic the natural distribution of 1-dehydro-6-gingerdione in ginger particles. Since no correlation can be identified between the curcumin, demethoxycurcumin and fluorescence lifetime, the variations of the phasor clouds were due to the presence of other fluorescence exhibited compounds, such as gingerol, shaogal and zingerone. Those compounds may also be present at high concentrations and even be the underlying cause. Therefore, it would be of interest to conduct a target analysis of all possible fluorescence exhibited compounds in ginger to further validate the reliability of FLIM.

4. Conclusions

To investigate the potential of applying Fluorescence Lifetime Imaging Microscopy (FLIM) to characterize ginger powder with different particle size, 15 powdered ginger and 30 smaller/larger-sized particle fractions generated from the 15 original samples were subjected to FLIM and pigment content analysis. The results indicated that FLIM possesses the capability to reflect the pigment information of ginger powder particles, while remaining unaffected by variations in particle size. Nonetheless, it is essential to overcome specific boundaries to advance future studies. Firstly, the phasor approach for comparative analysis of the population needs to be improved since the application of the average *g* and *s* values of each sample can only provide limited information on the fluorescence properties of samples. Secondly, the practical application of FLIM is inevitably hindered by the considerable experimental costs, presenting challenges for the implementation within the food industry. However, this study has proven the potential of FLIM in the characterization of spice powder and has demonstrated the prospects to expand to other food powders and provide new perspective to food quality analysis and/or authentication.

CRediT authorship contribution statement

Qing Han: . **Sara W. Erasmus:** Supervision, Validation, Writing – review & editing. **Arjen Bader:** . **Christos Fryganas:** . **Christopher T. Elliott:** Supervision, Writing – review & editing. **Saskia M. van Ruth:** Conceptualization, Funding acquisition, Project administration, Resources, Supervision, Writing – review & editing.

Declaration of competing interest

The authors declare that they have no known competing financial interests or personal relationships that could have appeared to influence the work reported in this paper.

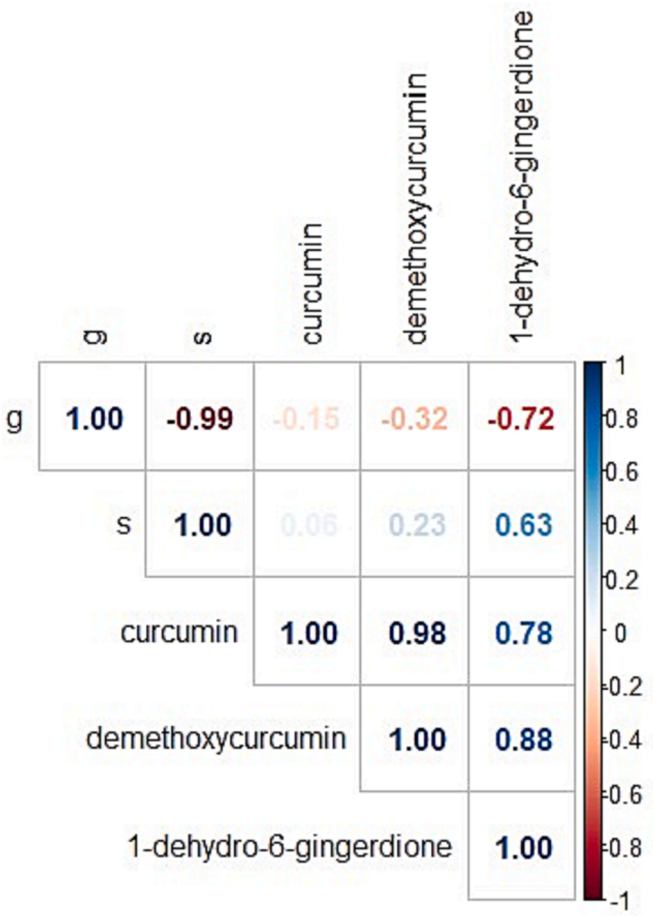

Fig. 8. Correlation analysis of fluorescence lifetime distribution and pigment compounds. Note: *g*: the real part of the Fourier transform of the fluorescence impulse response, *s*: the imaginary part of the Fourier transform of the fluorescence impulse response.

Data availability

Data will be made available on request.

Acknowledgements

This work was supported by China Scholarship Council, China (grant agreement No. 201903250123) and the EU-China-Safe project (http://www.euchinasafe.eu/) which is funded by the Horizon 2020 research and innovation programme, European Union, under grant agreement No. 727864. Any opinions, findings and conclusions or recommendations expressed in this material are that of the authors and the European Commission, European Union, does not accept any liability in this regard. The authors gratefully acknowledge all the companies for their participation in the study. We would also like to thank Jinzhou Jiang under the Master programme, Food Technology, Wageningen University & Research, Netherlands, for his help in the quantitative analysis of pigment compounds.

Appendix A. Supplementary data

Supplementary data to this article can be found online at https://doi.org/10.1016/j.foodres.2023.113792.

References

Ahmad, M. H., Sahar, A., & Hitzmann, B. (2017). Fluorescence Spectroscopy for the Monitoring of Food Processes. In *Measurement, Modeling and Automation in Advanced Food Processing* (pp. 121–151).

Amoah, R. E., Wireko-Manu, F. D., Oduro, I., Saalia, F. K., & Ellis, W. O. (2020). Effect of pretreatment on physicochemical, microbiological, and aflatoxin quality of solar sliced dried ginger (Zingiber officinale Roscoe) rhizome. *Food Science and Nutrition, 8*(11), 5934–5942. https://doi.org/10.1002/fsn3.1878

An, K., Wei, L., Fu, M., Cheng, L., Peng, J., & Wu, J. (2020). Effect of Carbonic Maceration (CM) on the Vacuum Microwave Drying of Chinese Ginger (Zingiber officinale Roscoe) Slices: Drying Characteristic, Moisture Migration, Antioxidant Activity, and Microstructure. *Food and Bioprocess Technology, 13*(9), 1661–1674. https://doi.org/10.1007/s11947-020-02504-y

Archana, Aman, A. K., Singh, R. K., & Nishant Kr., A. J. (2021). Effect of superfine grinding on structural, morphological and antioxidant properties of ginger (Zingiberofficinale) nano crystalline food powder. *Materials Today: Proceedings*, *43*, 3397–3403. https://doi.org/10.1016/j.jchromb.2008.01.011.

Chang, C. W., Sud, D., & Mycek, M. A. (2007). Fluorescence Lifetime Imaging Microscopy. *Methods in Cell Biology, 81*(06), 495–524. https://doi.org/10.1016/S0091-679X(06)81024-1

Coling, D., & Kachar, B. (1998). Principles and Application of Fluorescence Microscopy. *Current Protocols in Molecular Biology, 44*(1). https://doi.org/10.1002/0471142727.mb1410s44

Croce, A. C., & Bottiroli, G. (2014). Autofluorescence spectroscopy and imaging: A tool for biomedical research and diagnosis. *European Journal of Histochemistry, 58*(4), 320–337. https://doi.org/10.4081/ejh.2014.2461

Dhiman, A., & Prabhakar, P. K. (2021). Micronization in food processing: A comprehensive review of mechanistic approach, physicochemical, functional properties and self-stability of micronized food materials. *Journal of Food Engineering, 292*(April 2020), 110248. https://doi.org/10.1016/j.jfoodeng.2020.110248.

Digman, M. A., Caiolfa, V. R., Zamai, M., & Gratton, E. (2008). The phasor approach to fluorescence lifetime imaging analysis. *Biophysical Journal*, *94*(2), L14–L16. https://doi.org/10.1529/biophysj.107.120154.

Draszanowska, A., Karpińska-Tymoszczyk, M., & Olszewska, M. A. (2020). The effect of ginger rhizome and refrigerated storage time on the quality of pasteurized canned meat. *Food Science and Technology International, 26*(4), 300–310. https://doi.org/10.1177/1082013219889439

Dupuy, N., Le Dréau, Y., Ollivier, D., Artaud, J., Pinatel, C., & Kister, J. (2005). Origin of French virgin olive oil registered designation of origins predicted by chemometric analysis of synchronous excitation-emission fluorescence spectra. *Journal of Agricultural and Food Chemistry, 53*(24), 9361–9368. https://doi.org/10.1021/jf051716m

Fuliaş, A., Vlase, G., Vlase, T., Oneţiu, D., Doca, N., & Ledeţi, I. (2014). Thermal degradation of B-group vitamins: B1, B2 and B6: Kinetic study. *Journal of Thermal Analysis and Calorimetry, 118*(2), 1033–1038. https://doi.org/10.1007/s10973-014-3847-7

Gao, W., Chen, F., Wang, X., & Meng, Q. (2020). Recent advances in processing food powders by using superfine grinding techniques: A review. *Comprehensive Reviews in Food Science and Food Safety, 19*(4), 2222–2255. https://doi.org/10.1111/1541-4337.12580

Geverts, B., Van Royen, M. E., & Houtsmuller, A. B. (2014). Analysis of biomolecular dynamics by frap and computer simulation. In *Methods in Molecular Biology* (Vol. 1251). https://doi.org/10.1007/978-1-4939-2080-8_7.

Gomez-Perez, S. L., Haus, J. M., Sheean, P., Patel, B., Mar, W., Chaudhry, V., … Braunschweig, C. (2016). Measuring abdominal circumference and skeletal muscle from a single cross-sectional computed tomography image: A step-by-step guide for clinicians using National Institutes of Health ImageJ. *Journal of Parenteral and Enteral Nutrition, 40*(3), 308–318. https://doi.org/10.1177/0148607115604149

Hahn, D. W. (2009). *Light scattering theory*. University of Florida.

Han, Q., Peller, J., Erasmus, S. W., Elliott, C. T., & Van, S. M. (2023). Interpreting the variation in particle size of ground spice by high-resolution visual and spectral imaging : A ginger case study. *Food Research International*, *170*(December 2022), 113023. https://doi.org/10.1016/j.foodres.2023.113023.

Hao, S., Li, J., Liu, X., Yuan, J., Yuan, W., Tian, Y., & Xuan, H. (2021). Authentication of acacia honey using fluorescence spectroscopy. *Food Control, 130*(May), Article 108327. https://doi.org/10.1016/j.foodcont.2021.108327

Karoui, R., & Blecker, C. (2011). Fluorescence Spectroscopy Measurement for Quality Assessment of Food Systems-a Review. *Food and Bioprocess Technology, 4*(3), 364–386. https://doi.org/10.1007/s11947-010-0370-0

Keck, C. M., & Müller, R. H. (2008). Size analysis of submicron particles by laser diffractometry-90% of the published measurements are false. *International Journal of Pharmaceutics, 355*(1–2), 150–163. https://doi.org/10.1016/j.ijpharm.2007.12.004

Kubra, I. R., & Rao L, J. M. (2012). Microwave drying of ginger (Zingiber officinaleRoscoe) and its effects on polyphenolic content and antioxidant activity. *International Journal of Food Science and Technology, 47*(11), 2311–2317. https://doi.org/10.1111/j.1365-2621.2012.03104.x

Liang, J., Stöppelmann, F., Schoenbach, J., Rigling, M., Nedele, A. K., Zhang, Y., Hannemann, L., Hua, N., Heimbach, J., Kohlus, R., & Zhang, Y. (2023). Influence of peeling on volatile and non-volatile compounds responsible for aroma, sensory, and nutrition in ginger (Zingiber officinale). *Food Chemistry*, *419*(December 2022). https://doi.org/10.1016/j.foodchem.2023.136036.

Malacrida, L., Ranjit, S., Jameson, D. M., & Gratton, E. (2021). The Phasor Plot: A Universal Circle to Advance Fluorescence Lifetime Analysis and Interpretation. *Annual Review of Biophysics, 50*, 575–593. https://doi.org/10.1146/annurev-biophys-062920-063631

Marcu, L. (2012). Fluorescence lifetime techniques in medical applications. *Annals of Biomedical Engineering, 40*(2), 304–331. https://doi.org/10.1007/s10439-011-0495-y

Maslanka, R., Kwolek-Mirek, M., & Zadrag-Tecza, R. (2018). Autofluorescence of yeast Saccharomyces cerevisiae cells caused by glucose metabolism products and its methodological implications. *Journal of Microbiological Methods, 146*(January), 55–60. https://doi.org/10.1016/j.mimet.2018.01.017

Mekoue Nguela, J., Vernhet, A., Julien-Ortiz, A., Sieczkowski, N., & Mouret, J. R. (2019). Effect of grape must polyphenols on yeast metabolism during alcoholic fermentation. *Food Research International, 121*(March), 161–175. https://doi.org/10.1016/j.foodres.2019.03.038

Nasef, N. A., Loveday, S. M., Golding, M., Martins, R. N., Shah, T. M., Clarke, M., … Singh, H. (2019). Food matrix and co-presence of turmeric compounds influence bioavailability of curcumin in healthy humans. *Food and Function, 10*(8), 4584–4592. https://doi.org/10.1039/c9fo01063g

Perry, S. W., Burke, R. M., & Brown, E. B. (2012). Two-photon and second harmonic microscopy in clinical and translational cancer research. *Annals of Biomedical Engineering, 40*(2), 277–291. https://doi.org/10.1007/s10439-012-0512-9

Poudel, A., Pandey, J., & Lee, H. K. (2019). Geographical discrimination in curcuminoids content of turmeric assessed by rapid UPLC-DAD validated analytical method. *Molecules, 24*(9). https://doi.org/10.3390/molecules24091805

Ramesh, M. N., Wolf, W., Tevini, D., & Jung, G. (2001). Influence of processing parameters on the drying of spice paprika. *Journal of Food Engineering, 49*(1), 63–72. https://doi.org/10.1016/S0260-8774(00)00185-0

Rhodes, D. I., Sadek, M., & Stone, B. A. (2002). Hydroxycinnamic acids in walls of wheat aleurone cells. *Journal of Cereal Science, 36*(1), 67–81. https://doi.org/10.1006/jcrs.2001.0449

Rinnan, Å. (2014). Pre-processing in vibrational spectroscopy-when, why and how. *Analytical Methods, 6*(18), 7124–7129. https://doi.org/10.1039/c3ay42270d

Rodarmel, C., & Shan, J. (2002). Principal component analysis for hyperspectral image classification. *Surveying and Land Information Science, 62*(2), 115–122.

Sánchez, S. A., & Gratton, E. (2005). Lipid-protein interactions revealed by two-photon microscopy and fluorescence correlation spectroscopy. *Accounts of Chemical Research, 38*(6), 469–477. https://doi.org/10.1021/ar040026l

Sida, S., Samakradhamrongthai, R. S., & Utama-Ang, N. (2019). Influence of maturity and drying temperature on antioxidant activity and chemical compositions in ginger. *Current Applied Science and Technology, 19*(1), 28–42. https://doi.org/10.14456/cast.2019.4.

Sikorska, E., & Khmelinskii, I. (2016). Glowing colours of foods : Application of fluorescence and chemometrics in food studies. *Spectroscopy Europe, 28*(6), 10–13.

Stelzner, J., Roemhild, R., Garibay-Hernández, A., Harbaum-Piayda, B., Mock, H. P., & Bilger, W. (2019). Hydroxycinnamic acids in sunflower leaves serve as UV-A screening pigments. *Photochemical and Photobiological Sciences, 18*(7), 1649–1659. https://doi.org/10.1039/c8 pp00440d

Strege, S., Zetzener, H., & Kwade, A. (2013). From particle to powder properties-A mesoscopic approach combining micro-scale experiments and X-ray microtomography. *AIP Conference Proceedings*, *1542*(June 2007), 839–842. https://doi.org/10.1063/1.4812062.

Stringari, C., Cinquin, A., Cinquin, O., Digman, M. A., Donovan, P. J., & Gratton, E. (2011). Phasor approach to fluorescence lifetime microscopy distinguishes different metabolic states of germ cells in a live tissue. *Proceedings of the National Academy of Sciences of the United States of America, 108*(33), 13582–13587. https://doi.org/10.1073/pnas.1108161108

Tayyem, R. F., Heath, D. D., Al-Delaimy, W. K., & Rock, C. L. (2006). Curcumin content of turmeric and curry powders. *Nutrition and Cancer, 55*(2), 126–131. https://doi.org/10.1207/s15327914nc5502_2

Thennadil, S. N., & Martin, E. B. (2005). Empirical preprocessing methods and their impact on NIR calibrations: A simulation study. *Journal of Chemometrics, 19*(2), 77–89. https://doi.org/10.1002/cem.912

van Ruth, S., Dekker, P., Brouwer, E., Rozijn, M., Erasmus, S., & Fitzpatrick, D. (2019). The sound of salts by Broadband Acoustic Resonance Dissolution Spectroscopy. *Food Research International*. https://doi.org/10.1016/j.foodres.2018.09.044

Vedashree, M., Asha, M. R., Roopavati, C., & Naidu, M. M. (2020). Characterization of volatile components from ginger plant at maturity and its value addition to ice cream. *Journal of Food Science and Technology, 57*(9), 3371–3380. https://doi.org/10.1007/s13197-020-04370-0

Verma, V. K., Patel, R. K., Deshmukh, N. A., Jha, A. K., Ngachan, S. V., Singha, A. K., & Deka, B. C. (2019). Response of ginger and turmeric to organic versus traditional production practices at different elevations under humid subtropics of north-eastern India. *Industrial Crops and Products, 136*(May), 21–27. https://doi.org/10.1016/j.indcrop.2019.04.068

Vidot, K., Devaux, M. F., Alvarado, C., Guyot, S., Jamme, F., Gaillard, C., … Lahaye, M. (2019). Phenolic distribution in apple epidermal and outer cortex tissue by multispectral deep-UV autofluorescence cryo-imaging. *Plant Science, 283*(February), 51–59. https://doi.org/10.1016/j.plantsci.2019.02.003

Wan, X., Li, G., Zhang, M., Yan, W., He, G., Awelisah, Y. M., & Lin, L. (2020). A review on the strategies for reducing the non-linearity caused by scattering on spectrochemical quantitative analysis of complex solutions. *Applied Spectroscopy Reviews, 55*(5), 351–377. https://doi.org/10.1080/05704928.2019.1584567

Wang, H., Su, W., & Tan, M. (2020). Endogenous Fluorescence Carbon Dots Derived from Food Items. *Innovation, 1*(1), Article 100009. https://doi.org/10.1016/j.xinn.2020.04.009

Wang, K., Chi, G., Lau, R., & Chen, T. (2011). Multivariate calibration of near infrared spectroscopy in the presence of light scattering effect: A comparative study. *Analytical Letters, 44*(5), 824–836. https://doi.org/10.1080/00032711003789967

Weber, G. (1981). Resolution of the fluorescence lifetimes in a heterogeneous system by phase and modulation measurements. *The Journal of Physical Chemistry, 85*, 945–953. https://doi.org/10.1049/sbte005e_ch6

Yoko, I., & Aya, J. (2014). Pigment composition responsible for the pale yellow color of ginger (Zingiber officinale) rhizomes. *Food Science and Technology Research, 20*(5), 971–978. https://doi.org/10.3136/fstr.20.971

Zhao, X., Ao, Q., Du, F., Zhu, J., & Liu, J. (2010). Surface characterization of ginger powder examined by X-ray photoelectron spectroscopy and scanning electron microscopy. *Colloids and Surfaces B: Biointerfaces, 79*(2), 494–500. https://doi.org/10.1016/j.colsurfb.2010.05.019